

Prototyping of a LQG Compensator for a Compliant Positioning System with Friction

H. Henrichfreise
Cologne Laboratory of Mechatronics
Cologne University of Applied Sciences
hermann.henrichfreise@clm-online.de

Introduction

With increasing demands on speed and accuracy of positioning systems, friction and compliance, which are present in every mechanical system, have to be actively compensated by control. This requires abandoning the widespread classical (PI, PID) control concepts and apply approaches that are more advanced. A LQG (linear quadratic Gaussian) control is one method that is capable to do active vibration damping and disturbance (friction) compensation, allowing a high control bandwidth, strong disturbance rejection and precise positioning with rapid changes of speed and acceleration. If properly designed and implemented, a LQG control also shows a high robustness against external disturbances, nonlinear system behavior and plant parameter variations. Although control engineers have the theoretical background, which is well explained in most control design textbooks, e.g. [1,2], one can still hear arguing against LQG control with the more demanding theory, the complex computational tasks, the difficulty to find appropriate design parameters and the more demanding implementation issues. These arguments mostly originate from the lack of knowledge about the systematic procedure for design and implementation of a LQG control and about the extensive support given by recent development environments [3] for system modelling, analysis, design, simulation and rapid prototyping of control systems. In order to at least improve the knowledge about the procedure of LQG design and implementation, the aim of this paper is to show a straightforward approach for the position control of a compliant positioning system with friction. Since it has already been applied to other positioning devices, the approach can be seen as a sample for highly dynamical and precise position control design.

1. Compliant positioning system with friction

Fig. 1.1 shows the structure of the electromechanical positioning system (EMPS) which is used for experiments with position control at the Cologne Laboratory of Mechatronics (CLM).

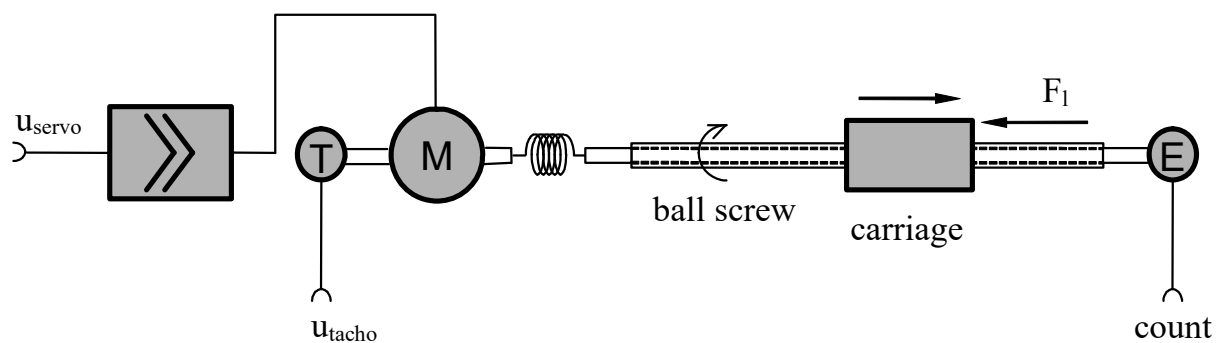


Fig. 1.1 Electromechanical positioning system (EMPS)

The EMPS consists of a DC motor with a current-controlled servo amplifier and a linear positioning unit. A backlash-free ball screw drive converts the rotatory motion of the motor to

the linear carriage displacement. A DC tachometer provides the velocity of the motor shaft, and an incremental encoder measures the carriage position. This is a standard configuration of drive systems in machine tools and gantry type robots. Compliance causing a mechanical resonance at about 100 Hz is added to the system by a flexible coupling between motor and positioning unit. The major source of dry friction is the ball screw drive. A pre-loading of the ball screw system, which is applied to avoid backlash, causes this friction. This configuration of the EMPS forms the plant.

To set up a mathematical model for control design, the mechanical part of the plant is described by a two degree of freedom rotatory system. Motor and tachometer build the drive-side moment of inertia J_d and the screw, the encoder as well as the carriage built the load-side moment of inertia J_l . The compliance between motor and positioning unit is modelled by a spring with stiffness c_{dl} and damping constant b_{dl} for material damping. Viscous friction is allocated to the drive and the load side by damping constants b_d and b_l . The dry friction in the ball screw drive is accounted for by an "internal" load-side friction torque M_{frl} . External forces F_l acting at the carriage, e.g. the cutting forces in a machine tool application, are taken care of by an extra torque input $M_l = F_l / i_s$, where i_s is the gear ratio of the ball screw unit. The system is driven by the motor torque M_d . The drive-side and load-side angular displacements φ_d and φ_l are selected as generalized coordinates. Then, the equations of motion for the mechanical part of the plant can be formulated as

$$\begin{aligned} J_d \ddot{\Omega}_d &= M_d - b_d \dot{\Omega}_d - b_{dl} (\dot{\Omega}_d - \dot{\Omega}_l) - c_{dl} (\varphi_d - \varphi_l) \\ J_l \ddot{\Omega}_l &= b_{dl} (\dot{\Omega}_d - \dot{\Omega}_l) + c_{dl} (\varphi_d - \varphi_l) - b_l \dot{\Omega}_l - (M_l + M_{frl}) \end{aligned} \quad (1.1a)$$

where $\Omega_d = \dot{\varphi}_d$ and $\Omega_l = \dot{\varphi}_l$. A simple model for the nonlinear dry friction including sticking, breakaway and sliding friction is formulated as

$$M_{frl} = \begin{cases} M_{extl} & \text{for } \Omega_l = 0 \wedge |M_{extl}| \leq M_{sl} \\ M_{sl} \operatorname{sgn}(M_{extl}) & \text{for } \Omega_l = 0 \wedge |M_{extl}| > M_{sl} \\ M_{Stribeck} (|\Omega_l|) \operatorname{sgn}(\Omega_l) & \text{for } \Omega_l \neq 0 \end{cases} \quad (1.1b)$$

where

$$M_{Stribeck}(\Omega) = M_{kl} + (M_{sl} - M_{kl}) e^{-\frac{\Omega}{\Omega_{Stribeck}}} \quad , \quad \Omega \geq 0 \quad (1.1c)$$

is a Stribeck characteristic with the maximum static (breakaway) friction M_{sl} , the constant level of kinetic friction M_{kl} (independent of velocity) and an exponential decay from static to kinetic friction according to the constant Stribeck velocity $\Omega_{Stribeck}$. In addition, the external torque M_{extl} acting at the inertia J_l is described by the equation

$$M_{extl} = c_{dl} (\varphi_d - \varphi_l) + b_{dl} (\dot{\Omega}_d - \dot{\Omega}_l) - b_l \dot{\Omega}_l - M_l \quad (1.1d)$$

A simple first order lag system

$$T_{servo} \dot{M}_d + M_d = k_{servo} (u_{servo} + v_{servo}) \quad (1.2)$$

with gain k_{servo} and time constant T_{servo} models the servo amplifier generating the motor torque M_d from the input voltage u_{servo} . This model also contains a disturbance input v_{servo} for servo amplifier noise.

The transducer behavior from the motor velocity Ω_d to the tachometer voltage u_{tacho} and from the screw displacement φ_1 to the value count of the incremental encoder counter are described by the equations

$$\begin{aligned} u_{\text{tacho}} &= k_{\text{corr}} (k_{\Omega} \Omega_d + u_{\text{ripple}}) + \mu_{\text{tacho}} + w_{\text{tacho}} \\ u_{\text{ripple}} &= r_{\text{ripple}} k_{\Omega} \Omega_d \left| \sin(\varphi_d n_{\text{ripple}}) \right| \\ k_{\text{corr}} &= \frac{1}{1 + r_{\text{ripple}} \frac{2}{\pi}} \end{aligned} \quad (1.3a)$$

and

$$\text{count} = \text{trunc}\left(2^{\text{bcount}-1} \frac{\varphi_1}{\varphi_{\text{max}}}\right) = \text{trunc}(k_{\varphi} \varphi_1) , \quad (1.3b)$$

where the terms $k_{\Omega} \Omega_d$ and $k_{\varphi} \varphi_1$ model the linear transducer properties. The gain $k_{\varphi} = 4 n_{\text{lines}} / (2 \pi)$ of the incremental encoder is given by the number n_{lines} of encoder lines and the line multiplication factor 4 (quadruple evaluation for the encoder lines). Nonlinear properties included in this model are an angular position-dependent ripple on the tachometer signal and the quantization characteristic of the incremental encoder, which have to be considered for precise position control. In equation (1.3a), the factor r_{ripple} builds the ripple amplitude from the undisturbed linear signal $k_{\Omega} \Omega_d$, and n_{ripple} describes the number of ripples per half turn of the tachometer shaft. The factor k_{corr} recovers the mean value of the ripple-free signal. The quantization of the incremental encoder signal is considered in equation (1.3b) by truncating the ideal real valued encoder signal to an integer value. Other measurement disturbances are the offset voltage μ_{tacho} and noise w_{tacho} on the tachometer signal.

Equations (1.1a) to (1.3b) have been implemented in a Simulink block diagram for simulation of the nonlinear control system with the LQG compensator described in the following section.

The linear plant model needed for compensator design has been derived by neglecting the nonlinear terms as well as the servo amplifier and measurement disturbances in the above equations. Choosing the angular positions φ_d and φ_1 , angular velocities Ω_d and Ω_1 as well as the motor torque M_d as state variables, the state space equations of the linear plant model with the state differential equation and measurement output equation become

$$\begin{aligned} \dot{\underline{x}}_p &= \underline{A}_p \underline{x}_p + \underline{B}_{pc} \underline{u}_{pc} + \underline{B}_{pd} \underline{u}_{pd} \\ \begin{bmatrix} \varphi_d \\ \Omega_d \\ \varphi_1 \\ \Omega_1 \\ M_d \end{bmatrix} &= \begin{bmatrix} 0 & 1 & 0 & 0 & 0 \\ -\frac{c_{dl}}{J_d} & -\frac{b_d + b_{dl}}{J_d} & \frac{c_{dl}}{J_d} & \frac{b_{dl}}{J_d} & \frac{1}{J_d} \\ 0 & 0 & 0 & 1 & 0 \\ \frac{c_{dl}}{J_1} & \frac{b_{dl}}{J_1} & -\frac{c_{dl}}{J_1} & -\frac{b_{dl} + b_1}{J_1} & 0 \\ 0 & 0 & 0 & 0 & -\frac{1}{T_{\text{servo}}} \end{bmatrix} \begin{bmatrix} \varphi_d \\ \Omega_d \\ \varphi_1 \\ \Omega_1 \\ M_d \end{bmatrix} + \begin{bmatrix} 0 \\ 0 \\ 0 \\ 0 \\ \frac{k_{\text{servo}}}{T_{\text{servo}}} \end{bmatrix} \underline{u}_{\text{servo}} + \begin{bmatrix} 0 \\ 0 \\ 0 \\ -\frac{1}{J_1} \\ 0 \end{bmatrix} (M_1 + M_{\text{fl}}) \end{aligned} \quad (1.4a)$$

and

$$\underline{y}_{pm} = \underline{C}_{pm} \underline{x}_p$$

$$\begin{bmatrix} \mathbf{u}_{\text{tacho}} \\ \text{count} \end{bmatrix} = \begin{bmatrix} 0 & k_{\Omega} & 0 & 0 & 0 \\ 0 & 0 & k_{\phi} & 0 & 0 \end{bmatrix} \begin{bmatrix} \phi_d \\ \Omega_d \\ \phi_l \\ \Omega_l \\ M_d \end{bmatrix}. \quad (1.4b)$$

Another equation needed for compensator design is the output equation

$$\underline{y}_{po} = \underline{C}_{po} \underline{x}_p + \underline{D}_{pod} \underline{u}_{pd}$$

$$\begin{bmatrix} \phi_l \\ \Omega_l \\ \alpha_l \end{bmatrix} = \begin{bmatrix} 0 & 0 & 1 & 0 & 0 \\ 0 & 0 & 0 & 1 & 0 \\ \frac{c_{dl}}{J_1} & \frac{b_{dl}}{J_1} & -\frac{c_{dl}}{J_1} & -\frac{b_{dl} + b_{ll}}{J_1} & 0 \end{bmatrix} \begin{bmatrix} \phi_d \\ \Omega_d \\ \phi_l \\ \Omega_l \\ M_d \end{bmatrix} + \begin{bmatrix} 0 \\ 0 \\ -\frac{1}{J_1} \end{bmatrix} (M_l + M_{frl}) \quad (1.4c)$$

for the objective variables of the plant, which are the load-side angular position ϕ_l , angular velocity Ω_l and angular acceleration α_l . They will be used to formulate the design objectives for the carriage motion.

The subscripts p, c, d, m, o at the above vectors and matrices stand for plant, control, disturbance, measurement and objective respectively.

The above equations are the basis for the design and closed-loop simulation of the LQG compensator which shall provide excellent reference behavior in the presence of disturbances from noise, external loads and internal friction. The corresponding linear and nonlinear model parameters, which are needed for the numerical evaluations, have been properly identified in [4]. A more comprehensive model with a detailed nonlinear modelling of the servo amplifier, load dependency and delayed friction in the friction model and additional drive-side friction is used in [5], which is however not required in the context of this paper.

2. LQG design

Different types of controllers have been designed for the EMPS, from a simple PID controller up to an output vector feedback with observer-based friction compensation [5,6]. The topic of this paper is the design and implementation of a LQG dynamic compensator for the linear plant model from equations (1.4a) to (1.4c). To include the operational environment of the control system, these equations are augmented by suitable linear models for reference and disturbance excitation. A weighting model is added to take into account engineering objectives in the design process. This approach and reasonable design parameters let the compensator outperform all the aforementioned control structures. The LQG compensator will be designed following the separation principle. First, a linear quadratic regulator (LQR) is designed for reference tracking and disturbance rejection, then a linear quadratic estimator (LQE) is added to provide the state variables for the regulator.

2.1 LQR design

To include the operational environment and the design objectives in the design process, equations (1.4a) and (1.4c) are taken for the linear plant model and are augmented by a reference excitation model

$$\begin{aligned} \dot{\underline{x}}_r &= \underline{A}_r \underline{x}_r, & \underline{x}_r(t=0) &= \underline{x}_{r0}, \\ \underline{y}_r &= \underline{C}_r \underline{x}_r, \end{aligned} \quad (2.1a)$$

a disturbance excitation model

$$\begin{aligned} \dot{\underline{x}}_d &= \underline{A}_d \underline{x}_d, & \underline{x}_d(t=0) &= \underline{x}_{d0}, \\ \underline{y}_d &= \underline{C}_d \underline{x}_d \end{aligned} \quad (2.1b)$$

and a weighting model

$$\begin{aligned} \dot{\underline{x}}_w &= \underline{A}_w \underline{x}_w + \underline{B}_{wr} \underline{u}_{wr} + \underline{B}_{wp} \underline{u}_{wp}, & \underline{x}_w(t=0) &= \underline{0} \\ \underline{y}_w &= \underline{C}_w \underline{x}_w + \underline{D}_{wr} \underline{u}_{wr} + \underline{D}_{wp} \underline{u}_{wp} \end{aligned} \quad (2.1c)$$

as shown in Fig. 2.1.

With the above models, as under real world conditions, the plant is considered to work in a mixed deterministic and stochastic environment [7].

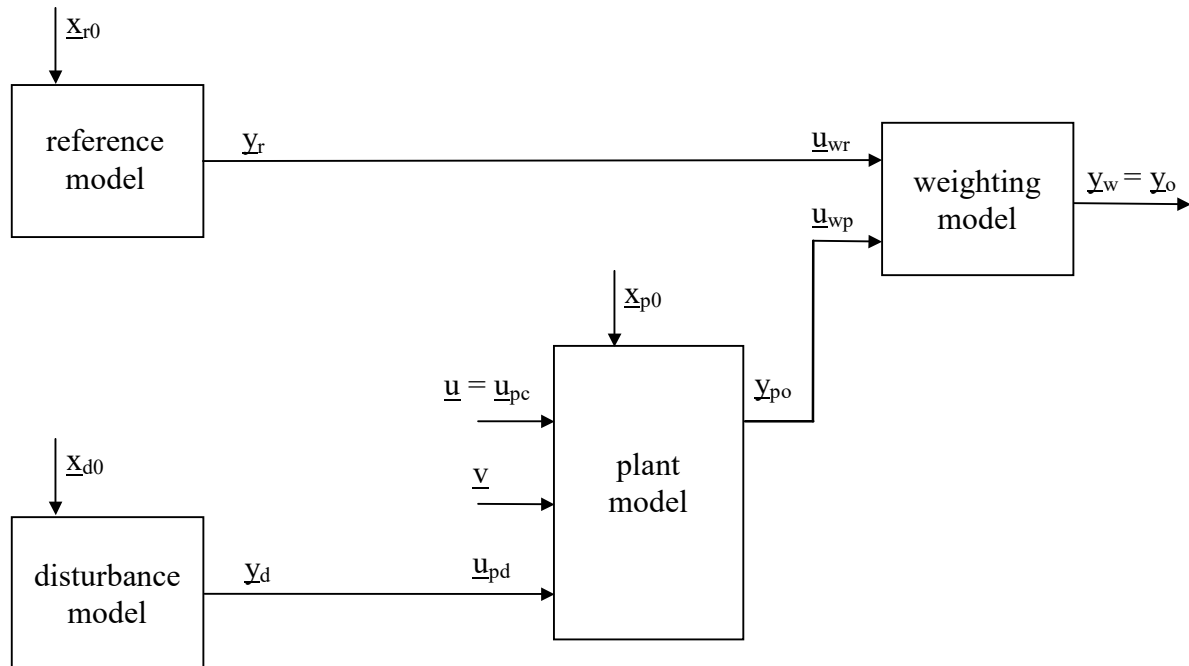


Fig. 2.1 Augmented plant model for LQR design

The deterministic environment of the plant is given by all signals whose shapes are known, but whose amplitudes can only be specified for a certain experiment. In Fig. 2.1, these signals are the reference and disturbance signals \underline{u}_{wr} and \underline{u}_{pd} . They are generated by the reference and disturbance models from appropriate initial conditions \underline{x}_{r0} and \underline{x}_{d0} of their state variables. To cover all possible experiments including varying initial conditions for the state variables of the plant, the initial conditions \underline{x}_{r0} , \underline{x}_{d0} and \underline{x}_{p0} are assumed to be unknown random variables with

zero mean, given variances and a Gaussian distribution. With this deterministic environment, it is easy to find appropriate model dynamics to generate the classes of time functions appearing under real operating conditions [7]. The fact that only their shapes have deterministic character while their amplitudes are random variables implies that the controlled system shall work for any meaningful amplitudes (initial conditions) and not only accurately track a single reference or reject a single disturbance torque profile.

In the following, the models for position control of the EMPS will be discussed.

A triple pseudo integrator

$$\begin{aligned} \dot{\underline{x}}_r &= \begin{bmatrix} -\frac{1}{T_r} & 1 & 0 \\ 0 & -\frac{1}{T_r} & 1 \\ 0 & 0 & -\frac{1}{T_r} \end{bmatrix} \underline{x}_r, \quad \underline{x}_r = \begin{bmatrix} \varphi_r \\ \Omega_r \\ \alpha_r \end{bmatrix}, \quad \underline{x}_r(t=0) = \underline{x}_{r0} \\ \underline{y}_r &= \begin{bmatrix} 1 & 0 & 0 \\ 0 & 1 & 0 \\ 0 & 0 & 1 \end{bmatrix} \underline{x}_r \end{aligned} \quad (2.2a)$$

is appropriate to generate step, ramp and parabolic position reference signals and their first and second derivatives for the elements of the output vector \underline{y}_r . With $T_r \rightarrow \infty$ tending to a true triple integrator, it provides the same type of output time functions from the initial conditions in the vector \underline{x}_{r0} as the reference profile generator in the final implementation of the control system.

If the disturbing torques at the input $u_{pd} = (M_l + M_{frl})$ of the plant are assumed to be step functions, which exactly models kinetic friction for $M_s = M_k$ in equations (1.1b) to (1.1d) and constant external loads, the disturbance model becomes the single pseudo integrator

$$\begin{aligned} \dot{x}_d &= -\frac{1}{T_d} x_d, \quad x_d(t=0) = x_{d0}, \\ y_d &= x_d \end{aligned} \quad (2.2b)$$

which corresponds to a true integrator for $T_d \rightarrow \infty$.

The need of pseudo integrators is imposed by the condition that the integral cost function for the LQR design must have a finite value, i.e. stable time responses of the contributing state variables for given initial conditions¹. Because the above state variables of the excitation models are not controllable from the input $\underline{u} = \underline{u}_{pc} = \underline{u}_{servo}$ of the plant (see Fig. 2.1) and hence cannot be stabilized by feedback, their integral behavior must be approximated by very slow first order systems which are called pseudo integrators. Their time constants have to be chosen far beyond the desired time constants of the closed-loop transient response. The results achieved from this approximation are numerically identical to those from the theoretical exact approach [8].

With the above definition of the deterministic environment, the stochastic environment of the plant is the remaining rest of all signals whose shapes and amplitudes are unknown. If nothing

¹ For white noise excitation, the integrand of the LQR cost function must become stationary.

is known about their spectral properties, these signals can be modelled as a zero-mean, Gaussian white noise vector process \underline{v} with constant intensity matrix \underline{V} disturbing the state variables of the plant (see Fig. 2.1). Otherwise, the respective signals could be modelled from white noise processes by the use of an appropriate linear filter model, which then as a noise disturbance model also becomes part of the augmented plant model. With the inclusion of this stochastic environment to the design process, it becomes clear that the LQR will be rejective to unknown disturbances and, to some extent, even to parameter variations in the real system. This rejectiveness is achieved with the design in the way that the influence of the disturbance signals to the LQR cost functions (see below) and thus to the corresponding controlled system time responses will be kept as small as possible with respect to the given design constraints, e.g. a limited control signal range.

Besides the modelling of the excitation of the plant, the other issue addressed in Fig. 2.1 is the formulation of engineering objectives. The weighting model

$$\underline{y}_w = \begin{bmatrix} e_\varphi \\ e_\Omega \\ e_\alpha \end{bmatrix} = \begin{bmatrix} 1 & 0 & 0 \\ 0 & 1 & 0 \\ 0 & 0 & 1 \end{bmatrix} \underline{u}_{wr} + \begin{bmatrix} -1 & 0 & 0 \\ 0 & -1 & 0 \\ 0 & 0 & -1 \end{bmatrix} \underline{u}_{wp} \quad (2.2c)$$

is used to build the design objective variables in the output vector \underline{y}_o of the augmented plant model. They are subject to the LQR design procedure. By using the errors e_φ , e_Ω and e_α of the load-side angular position φ_l , angular velocity Ω_l and angular acceleration α_l from the desired variables φ_r , Ω_r and α_r in the reference model output vector \underline{y}_r , the LQR design will yield steady-state accuracy for the considered class of reference and disturbance excitation by feedforward of the respective state variables of the reference and disturbance model.

Since it does not contain a state differential equation and does not contribute a state variable to the augmented plant model, the weighting model from equation (2.2c) performs a purely proportional weighting. With integral weighting of the position error the weighting model would look like

$$\dot{x}_w = 0 x_w + [1 \ 0 \ 0] \underline{u}_{wr} + [-1 \ 0 \ 0] \underline{u}_{wp}, \quad x_w(t=0) = 0$$

$$\underline{y}_w = \begin{bmatrix} e_\varphi \\ e_\Omega \\ e_\alpha \\ x_w \end{bmatrix} = \begin{bmatrix} 0 \\ 0 \\ 0 \\ 1 \end{bmatrix} x_w + \begin{bmatrix} 1 & 0 & 0 \\ 0 & 1 & 0 \\ 0 & 0 & 1 \\ 0 & 0 & 0 \end{bmatrix} \underline{u}_{wr} + \begin{bmatrix} -1 & 0 & 0 \\ 0 & -1 & 0 \\ 0 & 0 & -1 \\ 0 & 0 & 0 \end{bmatrix} \underline{u}_{wp}, \quad (2.2d)$$

which has been investigated for the EMPS position control in [9]. Feedback of the state variable x_w of the weighting model equals an integral state feedback, which is capable to produce steady-state accuracy for a constant signal at the disturbance input u_{pd} of the plant. Integral feedback is suitable for steady-state errors whose sources are not well known or are not easy to model or which cannot be compensated by other means. For the compensation of steady-state errors due to friction and external torques, the disturbance model and resulting state feedforward is preferable. Additional integral feedback may be useful if remaining errors are of the aforementioned type. Since for the EMPS the better results have been achieved with the disturbance model (2.2b) and the proportional weighting from equation (2.2c), this approach has been followed up in this paper.

With substitution of the input variables by the output variables corresponding to Fig. 2.1, the above models can be combined to the following state differential and objective output equation

$$\begin{aligned}\dot{\underline{x}} &= \underline{A}\underline{x} + \underline{B}\underline{u} + \underline{F}\underline{v}, \quad \underline{x}(t=0) = \underline{x}_0 \\ \underline{y}_o &= \underline{C}\underline{x}\end{aligned}\tag{2.3a}$$

of the augmented plant model for the LQR design [5], where for the general case

$$\underline{x} = \begin{bmatrix} \underline{x}_p \\ \underline{x}_r \\ \underline{x}_d \\ \underline{x}_w \end{bmatrix}, \quad \underline{u} = \underline{u}_{pc}, \quad \underline{y}_o = \underline{y}_w$$

$$\underline{A} = \begin{bmatrix} \underline{A}_p & \underline{0} & \underline{B}_{pd}\underline{C}_d & \underline{0} \\ \underline{0} & \underline{A}_r & \underline{0} & \underline{0} \\ \underline{0} & \underline{0} & \underline{A}_d & \underline{0} \\ \underline{B}_{wp}\underline{C}_{po} & \underline{B}_{wr}\underline{C}_r & \underline{B}_{wp}\underline{D}_{pod}\underline{C}_d & \underline{A}_w \end{bmatrix}, \quad \underline{B} = \begin{bmatrix} \underline{B}_{pc} \\ \underline{0} \\ \underline{0} \\ \underline{0} \end{bmatrix}, \quad \underline{F} = \begin{bmatrix} \underline{F}_p \\ \underline{0} \\ \underline{0} \\ \underline{0} \end{bmatrix}$$

and

$$\underline{C} = \begin{bmatrix} \underline{D}_{wp}\underline{C}_{po} & \underline{D}_{wr}\underline{C}_r & \underline{D}_{wp}\underline{D}_{pod}\underline{C}_d & \underline{C}_w \end{bmatrix} .\tag{2.3b}$$

The LQR design for this model provides the gain matrix \underline{K} for the optimal linear regulator

$$\underline{u} = -\underline{K}\underline{x} = -\begin{bmatrix} \underline{K}_p & \underline{K}_r & \underline{K}_d & \underline{K}_w \end{bmatrix} \begin{bmatrix} \underline{x}_p \\ \underline{x}_r \\ \underline{x}_d \\ \underline{x}_w \end{bmatrix}\tag{2.4}$$

including feedforward of the state variables of the reference and disturbance model by the gain submatrices \underline{K}_r and \underline{K}_d as well as feedback of the state variables of the plant and weighting model by the matrices \underline{K}_p and \underline{K}_w . While the feedforward provides steady-state accuracy for the modelled classes of reference and disturbance signals, the feedback of the state variables of the plant and weighting model stabilizes unstable modes and produces a fast and well-damped decay of the transient errors.

The optimal regulator minimizes the quadratic cost functions (2.5a) and (2.5b) built by the weighted engineering objectives from the output vector \underline{y}_o and the weighted control input \underline{u} of the plant. They are the expected value of the steady-state ($t \rightarrow \infty$) integral

$$J = E \left\{ \lim_{t \rightarrow \infty} \int_0^t (\underline{y}_o^T \underline{Q} \underline{y}_o + \underline{u}^T \underline{R} \underline{u}) d\tau \right\}\tag{2.5a}$$

for the system excited from the deterministic environment or the steady-state expected value

$$J = \lim_{t \rightarrow \infty} E \{ \underline{y}_o^T \underline{Q} \underline{y}_o + \underline{u}^T \underline{R} \underline{u} \}\tag{2.5b}$$

of the integrand itself for excitation from the stochastic environment, where the symmetric weighting matrices \underline{Q} and \underline{R} have to be positive semi-definite and positive definite respectively. With diagonal weighting matrices $\underline{Q} = \text{diag}(q_{e_\phi}, q_{e_\Omega}, q_{e_a})$ and $\underline{R} \rightarrow r_{u_{\text{servo}}}$ as well as the actual

objective variables e_ϕ , e_Ω and e_α for proportional weighting from (2.2c) and the control input u_{servo} , the quadratic forms in the above cost functions become

$$\underline{y}_o^T \underline{Q} \underline{y}_o + \underline{u}^T \underline{R} \underline{u} = q_{e_\phi} e_\phi^2 + q_{e_\Omega} e_\Omega^2 + q_{e_\alpha} e_\alpha^2 + r_{u_{\text{servo}}} u_{\text{servo}}^2 \quad (2.5c)$$

Consequently, the first cost function can be interpreted as the expected value of the weighted sum of the mean square amplitudes of the variables for random initial conditions (only factor $1/t$ before the integral is missing). The second function represents the weighted sum of the steady-state covariances for noise excitation.

It makes no difference for the result of the LQR design which case of environment and corresponding cost function is considered. For both cases the optimal gain matrix is given by

$$\underline{K} = \underline{R}^{-1} \underline{B}^T \underline{S} \quad (2.5d)$$

where the matrix \underline{S} is the positive definite solution of the algebraic Riccati equation

$$\underline{S} \underline{A} + \underline{A}^T \underline{S} - \underline{S} \underline{B} \underline{R}^{-1} \underline{B}^T \underline{S} + \underline{C}^T \underline{Q} \underline{C} = \underline{0} \quad (2.5e)$$

for the augmented plant model from equation (2.3a) [1,7]. Since the gain matrix and thus the optimal regulator does neither depend on the noise injection matrix \underline{F} nor on the intensity matrix \underline{V} of the white noise process \underline{v} in equation (2.3a), the control is optimal for any noise excitation \underline{v} of the state variables of the augmented plant model. The LQR design task given by equations (2.5d) and (2.5e) can be solved with the MATLAB Control System Toolbox [10]. Due to the linearly dependent eigenvectors associated with the pseudo integrator eigenvalues in the reference model, a function basing on a Schur algorithm [11] has to be used and modified for the cost function with weighted outputs.

The design parameters still missing for the computation of the optimal gain matrix are the weightings q_{e_ϕ} , q_{e_Ω} , q_{e_α} and $r_{u_{\text{servo}}}$ which for deterministic excitation tune the controlled system behavior by penalizing large amplitudes and slow decay of the objective variables and too extensive use of the control signal. Now, the question is how to determine suitable, physically meaningful values.

If the quadratic terms in (2.5c) are interpreted as variance contributions of the individual time functions to the final cost J , one can see that the reciprocal values of the maximum allowed variances σ_i^2 for the individual signals are suitable weighting values. Applied to equation (2.5c) the quadratic forms become

$$\underline{y}_o^T \underline{Q} \underline{y}_o + \underline{u}^T \underline{R} \underline{u} = \frac{1}{\sigma_{e_\phi}^2} e_\phi^2 + \frac{1}{\sigma_{e_\Omega}^2} e_\Omega^2 + \frac{1}{\sigma_{e_\alpha}^2} e_\alpha^2 + \frac{1}{\sigma_{u_{\text{servo}}}^2} u_{\text{servo}}^2 \quad (2.6)$$

From this equation, it can be concluded that the smaller a maximum allowed variance the higher the corresponding weighting, i.e. the penalty on the variance contribution of the respective signal to the final cost value. Because the random variables from the design environment are assumed to be Gaussian (normally) distributed, this is also valid for the input and output signals u_{servo} , e_ϕ , e_Ω and e_α of the augmented plant model. For zero mean values, this implies that their ranges are covered to approximately 99% by three times the individual standard deviations σ_i . Therefore, the values σ_i for the weightings in equation (2.6) can be set to one third of the maximum allowed absolute signal values. The resulting weightings $1/\sigma_i^2$ scale the values and units of the variance contributions in equation (2.6) for the given constraints of the

corresponding time functions. For example, if the control signal u_{servo} has a range of ± 10 V and the EMPS's rigid body acceleration has a range of ± 15000 rad / s², whereas the position error e_φ shall stay in a range of ± 0.15 rad (± 60 μm), the respective weightings become

$$r_{u_{\text{servo}}} = 0.09 / \text{V}^2, \quad q_{e_\alpha} = 0.0002 \text{ sec}^4 / \text{rad}^2, \quad q_{e_\varphi} = 400 / \text{rad}^2.$$

Following the above rule for the weightings of the cost functions from the equations (2.5a) and (2.5b), the LQR design for the EMPS provides good time responses right from the design start. Minor fine-tuning of the output weightings is necessary when adding the estimator after the second design step in order to improve the final closed-loop system time responses with the compensator.

After having found the LQR gain matrix, one has to consider that not all state variables from the augmented plant model in Fig. 2.1 can be measured or computed from feedforward commands. The only signals available are the state variables of the reference model, which can be taken from the reference profile generator as a standard part of every position control application, and the state variables of the weighting model, which can be computed from the inputs of the regulator and the given weighting model dynamics (see section 2.3). Therefore, an estimator is required for the state variables of the plant and disturbance model. Indeed, the state variables Ω_d and φ_1 of the plant could be computed from the measurement variables (equation (1.4b)), but they are affected by quantization as well as noise, and need some filtering by the estimator.

The design of the estimator, which provides smooth and optimum estimates for the state variables of the plant and disturbance model, is the topic of the next, second design step.

2.2 LQE design

The linear plant model with the state differential equation (1.4a) and measurement output equation (1.4b) is needed for the LQE design. The linear disturbance model

$$\begin{aligned} \dot{\underline{x}}_d &= \underline{A}_d \underline{x}_d + \underline{B}_d \underline{u}_d, \quad \underline{x}_d(t=0) = \underline{0} \\ \underline{y}_d &= \underline{C}_d \underline{x}_d \end{aligned} \tag{2.7a}$$

with unknown input \underline{u}_d is added as shown in Fig. 2.2 to include the deterministic disturbance environment in the estimator. As already discussed for the LQR design, an integrator model

$$\begin{aligned} \dot{\underline{x}}_d &= \underline{u}_d, \quad \underline{x}_d(t=0) = 0 \\ \underline{y}_d &= \underline{x}_d \end{aligned} \tag{2.7b}$$

is suitable to generate step-shaped disturbance signals for the disturbance input $u_{pd} = (M_l + M_{frl})$ of the EMPS. One can assume Dirac pulses with random pulse weight at the disturbance input u_d to get a step-shaped output y_d , which is equivalent to the initial condition for the state variable of the disturbance model used for the LQR design. The fact that this deterministic input cannot be measured like the other input and output signals from Fig. 2.2 will be accounted for when specifying the corresponding intensity in the LQE design. Contrarily to the LQR design, there will be no problem with the pure integrator for the LQE design, if the state of the disturbance model in the augmented plant model is observable and controllable (see below).

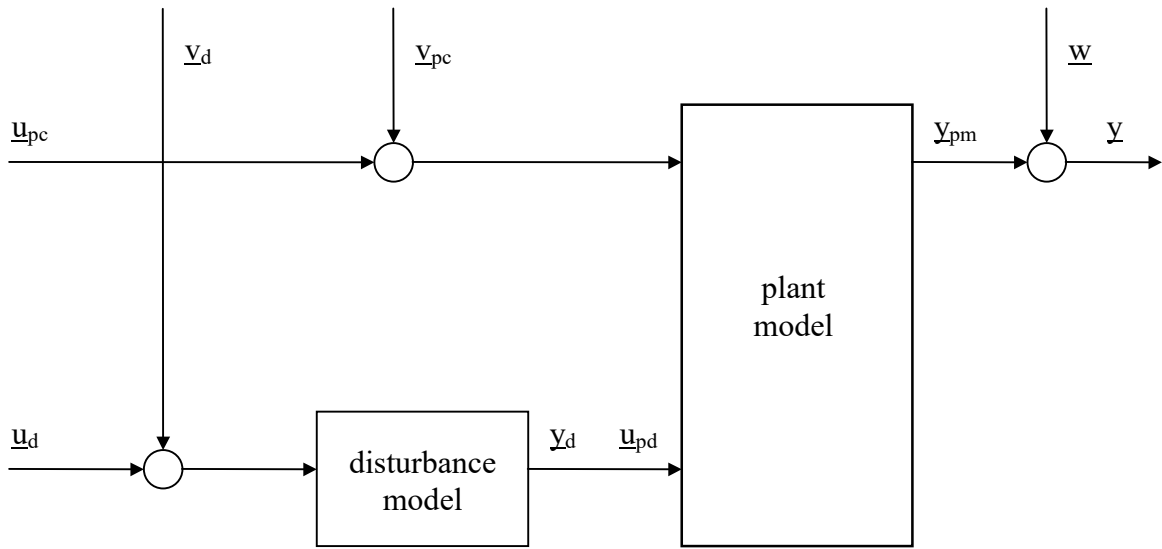


Fig. 2.2 Augmented plant model for LQE design

The stochastic environment of the plant model is given by the vector process \underline{v} for process noise and the vector process \underline{w} for measurement noise.

With substitution of the disturbance input vector \underline{u}_{pd} by the output vector \underline{y}_d of the disturbance model from equation (2.7a) and consideration of the noise processes corresponding to Fig. 2.2, the augmented plant model for the LQE design becomes [5]

$$\begin{aligned} \dot{\underline{x}} &= \underline{A} \underline{x} + \underline{B} \underline{u} + \underline{B} \underline{v} \\ \underline{y} &= \underline{y}_{pm} + \underline{w} = \underline{C} \underline{x} + \underline{w} \end{aligned} \quad (2.8a)$$

where for the general case

$$\begin{aligned} \underline{x} &= \begin{bmatrix} \underline{x}_p \\ \underline{x}_d \end{bmatrix}, \quad \underline{u} = \begin{bmatrix} \underline{u}_{pc} \\ \underline{u}_d \end{bmatrix}, \quad \underline{v} = \begin{bmatrix} \underline{v}_{pc} \\ \underline{v}_d \end{bmatrix} \\ \underline{A} &= \begin{bmatrix} \underline{A}_p & \underline{B}_{pd} \underline{C}_d \\ \underline{0} & \underline{A}_d \end{bmatrix}, \quad \underline{B} = \begin{bmatrix} \underline{B}_{pc} & \underline{0} \\ \underline{0} & \underline{B}_d \end{bmatrix} \quad \text{and} \quad \underline{C} = \begin{bmatrix} \underline{C}_{pm} & \underline{0} \end{bmatrix}. \end{aligned} \quad (2.8b)$$

It is required for the LQE design that all state variables are observable in the measurement output vector \underline{y} of the plant and controllable by the process noise input vector \underline{v} of the augmented plant model.

Injection of the vector process \underline{v} of process noise by the same input matrix \underline{B} as used for the input vector \underline{u} , i.e. directly at the input of the augmented plant model, is in preparation for trying to achieve loop transfer recovery (LTR) with the LQE design.

Considering Fig. 2.3, the objective of the LQE design becomes the following: Find the best estimates for the noisy or unknown state variables of the plant and for the unknown state variables of the disturbance model contained in the augmented state vector \underline{x} of the plant in the presence of process and measurement noise. Consequently, for a high level of process noise and a low level of measurement noise, the estimator has to rely on the measurements rather than on the input signals and vice versa.

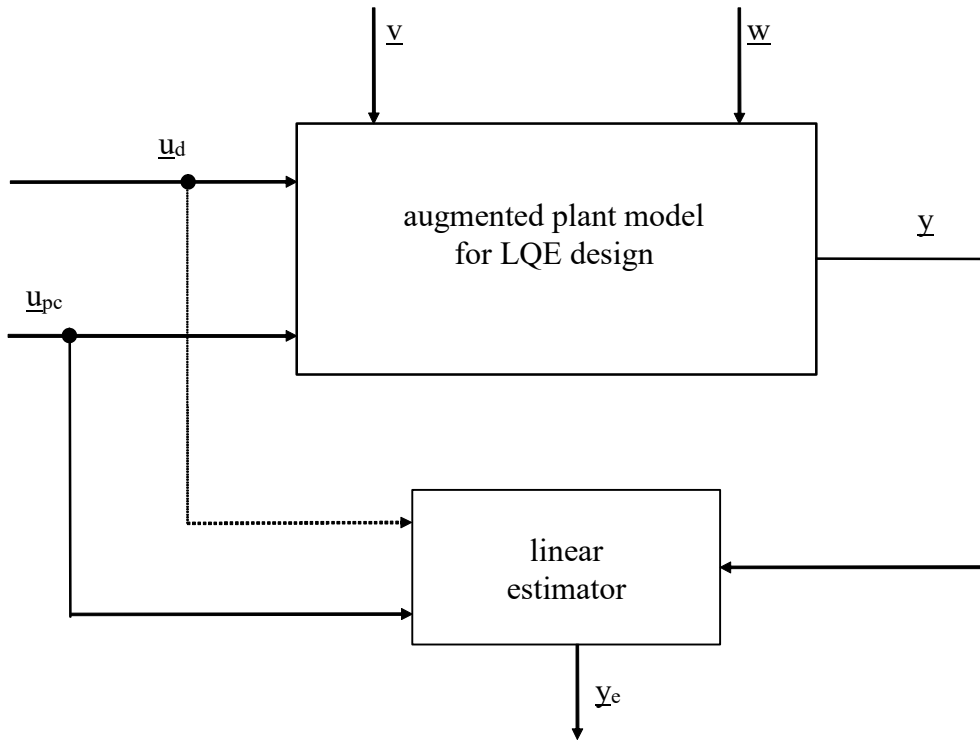


Fig. 2.3 *Augmented plant model with linear estimator*

If the vector process \underline{v} for process noise and the vector process \underline{w} for measurement noise are assumed to be stationary, zero-mean, Gaussian white noise processes with known constant symmetric intensity matrices \underline{V} and \underline{W} , the optimal estimator for the augmented plant model from equation (2.8a) is given by the linear state space equations

$$\begin{aligned} \dot{\hat{\underline{x}}} &= (\underline{A} - \underline{L}\underline{C})\hat{\underline{x}} + \underline{B}\underline{u} + \underline{L}\underline{y} \\ \underline{y}_e &= \hat{\underline{x}} \end{aligned} \quad (2.9)$$

This optimal estimator minimizes the cost function

$$J = \lim_{t \rightarrow \infty} E\{(\underline{x} - \hat{\underline{x}})^T (\underline{x} - \hat{\underline{x}})\} \quad (2.10a)$$

for the estimation error $\underline{x} - \hat{\underline{x}}$, i.e. the sum of the steady-state ($t \rightarrow \infty$) autocovariances of the estimation error. Then, the LQE design provides the optimal estimator gain matrix

$$\underline{L} = \underline{P}\underline{C}^T \underline{W}^{-1} \quad (2.10b)$$

where the optimal steady-state covariance matrix \underline{P} of the estimation error is the positive definite solution of the algebraic Riccati equation

$$\underline{A}\underline{P} + \underline{P}\underline{A}^T - \underline{P}\underline{C}^T \underline{W}^{-1} \underline{C}\underline{P} + \underline{B}\underline{V}\underline{B}^T = \underline{0} \quad (2.10c)$$

However, since the disturbance input \underline{u}_d is not available in reality, the estimator is implemented with the state differential equation

$$\dot{\hat{\underline{x}}} = (\underline{A} - \underline{L}\underline{C})\hat{\underline{x}} + \underline{B}_e \underline{u}_{pc} + \underline{L}\underline{y} \quad (2.11)$$

where \underline{B}_e is the left hyper-column of \underline{B} from equation (2.8b).

The design task given by equations (2.10b) and (2.10c) can be easily solved by using the corresponding functions from the MATLAB Control System Toolbox.

Meaningful intensity matrices \underline{V} and \underline{W} are needed as the design parameters for the LQE design to compute the estimator gain matrix. These matrices have a similar meaning as the weighting matrices from the LQR design, because they penalize the usage of the inputs and outputs of the augmented plant model for the estimation of the augmented state vector \underline{x} (see Fig. 2.2). The task of specifying numerical values for the intensity matrices simplifies if the individual elements of the vector processes \underline{v} and \underline{w} are assumed to be uncorrelated, so that the intensity matrices $\underline{V} = \text{diag}(V_{ii})$ and $\underline{W} = \text{diag}(W_{ii})$ become diagonal.

With a closer look at the signals, as the estimator in the later digital implementation will see them, one can derive a simple rule to specify values for the remaining diagonal elements. We consider that all measurement signals are sampled with the sampling period T_s and, if they are not already digital like the encoder signal, are converted to digital by A/D-converters. Since the A/D-converters and the encoder have a limited resolution (word length or number of lines), the values at the sampling instants are subject to quantization. The resulting errors can be modelled as uniformly distributed discrete white noise processes that are added to the sampled measurement signals [12]. This so-called quantization noise has a variance of

$$\sigma_i^2 = \frac{1}{12} \Delta_i^2 = \frac{1}{3} 2^{-2b_i} A_i^2, \quad (2.12a)$$

$$A_i = 2^{b_i-1} \Delta_i$$

where Δ_i is the quantization step size, b_i the word length and $\pm A_i$ the analog range of the converter. Since it is discrete white noise, the spectral density function $S_i(\omega)$ of the quantization noise has a constant intensity σ_i^2 and is defined in the frequency range of $\pm \pi / T_s$. The discrete white noise approaches the continuous white noise spectral density function in the limit as T_s approaches zero, if σ_i^2 is set to W_{ii} / T_s [2].

Thus, if quantization noise is the only noise source for the measurement signals, which is the case for the encoder signal, suitable values for intensities of the continuous white noise processes for the LQE design are

$$W_{ii} = \sigma_i^2 T_s. \quad (2.12b)$$

Since a common factor in the intensities does not affect the result of the LQE design, there is no need to decide on a sampling period in this stage of the design. Therefore, the LQE design parameters can be set to $W_{ii} = \sigma_i^2$.

Following the above rule, the noise intensity for the incremental encoder signal with a quantization step size of $\Delta_{\text{count}} = 1$ becomes $W_{22} = \sigma_{\text{count}}^2 = 1/12$. Measurement noise not resulting from quantization (e.g. from the measurement transducers and amplifiers) can be taken into account by an equivalent quantization noise process, i.e. by decreasing the converter word length to an effective number of bits $b = b_{\text{eff}}$ which could be calculated from equation (2.12a) with a real noise variance measurement. Of course, a variance measurement could directly be used as a design parameter instead.

A quick way to plug in suitable values for the design parameters is to set the quantization step size Δ_i to the range of the measured signal noise floor and use equation (2.12a) for the variance. With a noise floor of ± 0.01 V on the tachometer signal, $\Delta_{\text{tachometer}}$ becomes 0.02 V, which results in $W_{11} = \sigma_{\text{tachometer}}^2 = 3.33 \cdot 10^{-5} \text{ V}^2$. This value corresponds to an effective number of bits of about 10.

A first guess for the intensities V_{ii} of the process noise at the control input of the plant, which is caused by the D/A-converter of the compensator at its output, can also be found according to equation (2.12a). Again, noise not resulting from D/A-quantization (e.g. from the servo amplifier) can be taken into account by appropriately setting the quantization step size Δ_i . The resulting variance value needs additional increase to improve the robustness of the closed-loop system with the estimator by trying to achieve loop transfer recovery [1,2,13].

With increasing intensities for the process noise, the eigenvalues of the estimator tend to the transmission zeros of the augmented plant model from equation (2.8a) and to infinity. Thus, the intensities are limited due to the eigenvalues of the estimator becoming too fast for implementation or tending to unfavorably located transmission zeros (e.g. near the origin of the s-plane)². The limiting matter for the EMPS is a transmission zero of equation (2.8a) in the origin of the s-plane. If the intensity for process noise is selected too high, the eigenvalue tending to zero leads to an unsatisfying disturbance behavior. This becomes visible by a very slow mode in the time response of the closed-loop system for a step at the disturbance input M_i of the plant.

Since the disturbance input \underline{u}_d of the augmented plant model is unknown and cannot be measured, the intensities of the corresponding noise process have to be selected as high as possible to make the estimator robust against the fact that the signal is missing for implementation. Again, implementation constraints determine the intensity limits: The frequencies of the estimator eigenvalues should be kept about three to ten times below the implementation sampling frequency $f_s = 1 / T_s$ of the compensator.

After having discussed the proper selection of the noise intensities as LQE design parameters, let's have a closer look on the meaning of loop transfer recovery with the illustration given in Fig. 2.4. If the control loop is cut directly before the control input of the plant, the estimator will receive a wrong input (output \underline{y}_{LQG} of the compensator instead of input \underline{u}_{pc} of the plant). If the compensator is poorly designed, it may even become unstable due to the feedback of its output to the input of the estimator. To achieve both robustness to a wrong input and stability, the estimator has to be designed in such a way that it does not need the control input of the plant or at least is not overly dependent on it. This is achieved by increasing the intensities of the process noise at the control input of the plant in the LQE design. As the intensities for the process noise are tending towards infinity, the output of the compensator is no longer needed as an input of the estimator. The augmented state vector \underline{x} of the plant is solely reconstructed from the measurement output \underline{y}_{pm} of the plant, so that the estimator inverts the measurement output equation of the plant. If this estimator is assumed shifted to the subsystem of the plant, it can be recognized that the open-loop transfer path from the control input \underline{u}_{pc} of the plant to the output \underline{y}_{LQG} of the LQG compensator recovers the loop transfer path (LTR) from \underline{u}_{pc} to the output \underline{y}_{LQR} of the static state feedback regulator. This also recovers the very good robustness properties of the control system with LQR, i.e. static state feedback only. It has an infinite gain margin and a phase margin of at least 60° [2]. For the considered transfer path, the dynamics of the estimator are no longer relevant.

² If transmission zeros are located in the right half of the s-plane, the eigenvalues tend to their reflection relative to the imaginary axis.

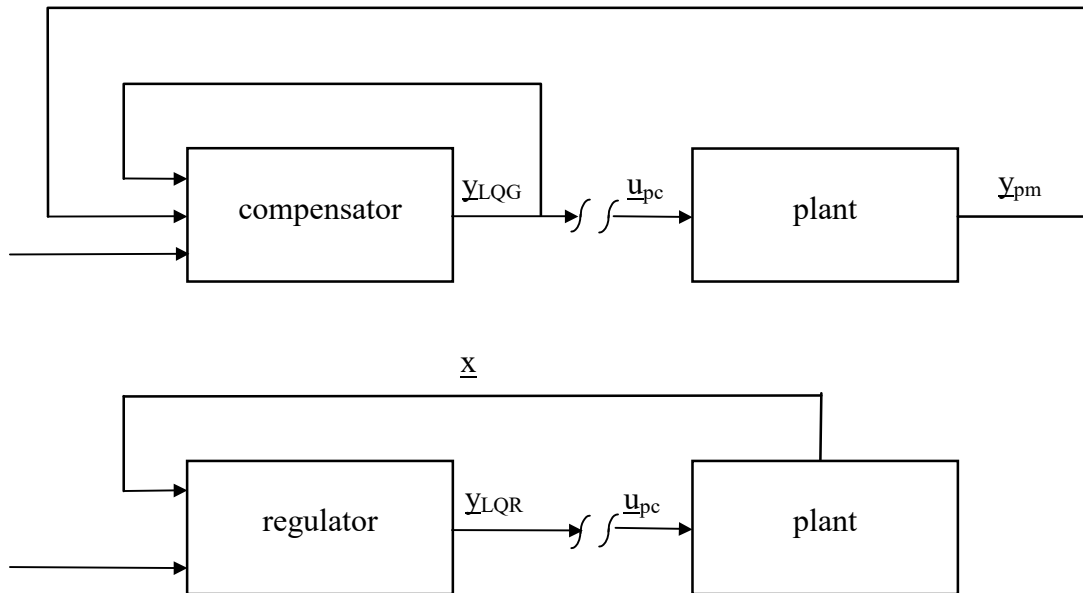


Fig. 2.4 *Meaning of LTR*

For a single control input of the plant, the grade of LTR can be easily assessed by comparing the open-loop frequency response of the systems from Fig. 2.4. Singular value frequency responses are required for multiple control inputs. They can be computed with a function from the MATLAB Control System Toolbox.

2.3 Assembly of LQG compensator

After the design of the optimal regulator and optimal estimator as described in the previous sections, the LQG compensator can be assembled as shown in Fig. 2.5 and Fig. 2.6.

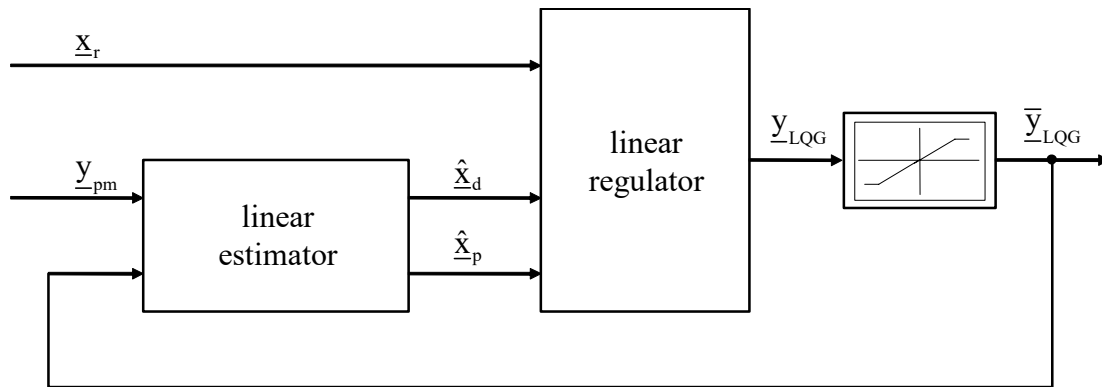


Fig. 2.5 *Compensator with regulator and estimator*

Since for implementation the reference model from the design structure will be replaced by a reference profile generator, the vector \underline{x}_r containing the load-side reference angular position φ_r , angular velocity Ω_r and angular acceleration α_r (see equation (2.2a)) becomes an input of the regulator. These signals will be derived from the corresponding reference signal for the linear carriage motion by division by the gear ratio i_s of the ball screw unit. The other inputs of the regulator are the estimate $\hat{\underline{x}}_d$ of the state vector of the disturbance model and the estimate $\hat{\underline{x}}_p$ of the state vector of the plant provided by the estimator (see equation (2.9) resp. (2.11)). Since the disturbance input \underline{u}_d of the estimator cannot be measured, it has been omitted. As mentioned in the LQE design section, the estimator has been designed robust for this. The saturation block before the compensator output and in the feedback to the input of the estimator is included to

improve the estimates of the state variables when actuator saturations become effective in the control input path of the plant [14]. Its bounds are set equal to the maximum current limits of the servo amplifier so that the estimator will get a correct input signal if the control input signal of the plant is saturated at these bounds. Due to LTR, the estimator and thus the control system behave robust when the current limits or the voltage limits are hit inside the amplifier. The subsystem of the regulator is assembled according to equation (2.4). It is shown in Fig. 2.6.

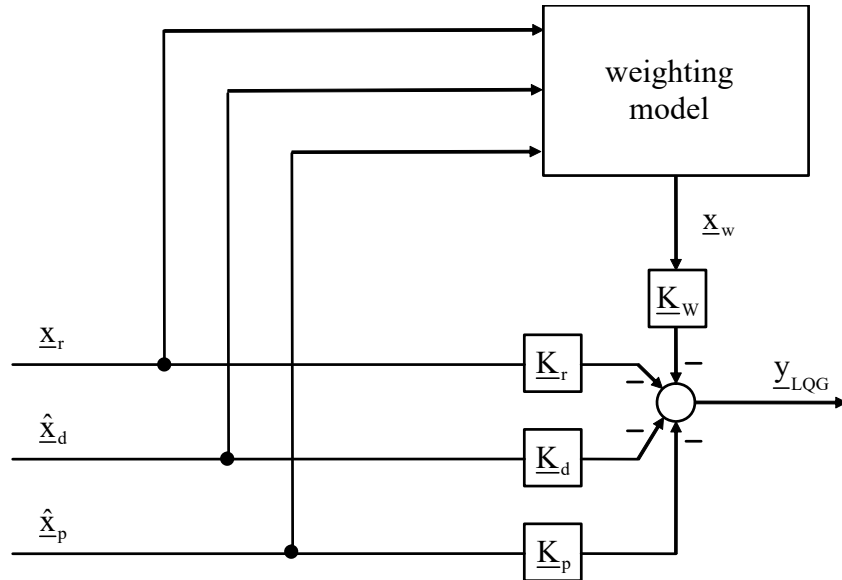


Fig. 2.6 Regulator with weighting model

If the weighting model in the augmented plant model for the LQR design from Fig. 2.1 contributes a state vector \underline{x}_w , the corresponding dynamics

$$\dot{\underline{x}}_w = \underline{A}_w \underline{x}_w + \underline{B}_{wr} \underline{C}_r \underline{x}_r + \underline{B}_{wp} (\underline{C}_{po} \hat{\underline{x}}_p + \underline{D}_{pod} \underline{C}_d \hat{\underline{x}}_d) \quad (2.13a)$$

and their contribution to the output of the regulator

$$\underline{y}_{k_w} = \underline{K}_w \underline{x}_w \quad (2.13b)$$

have to be added to the block diagram of the regulator as in Fig. 2.6. This would be the case for integral weighting with the model from equation (2.2d). For purely proportional weighting with the model from equation (2.2c), which has been used for the LQR design, the upper part of Fig. 2.6 has to be omitted.

The above compensator has been analyzed with the plant model for iterative fine-tuning of the LQR/LQE design parameters to improve the final closed-loop system behavior. One of the analysis steps is the assessment of the robustness of the linear control system by comparing the frequency responses of the LQR and LQG controlled open-loop systems from Fig. 2.4 for LTR. Fig. 2.7 shows these frequency responses for the final compensator design. LTR has been sufficiently achieved.

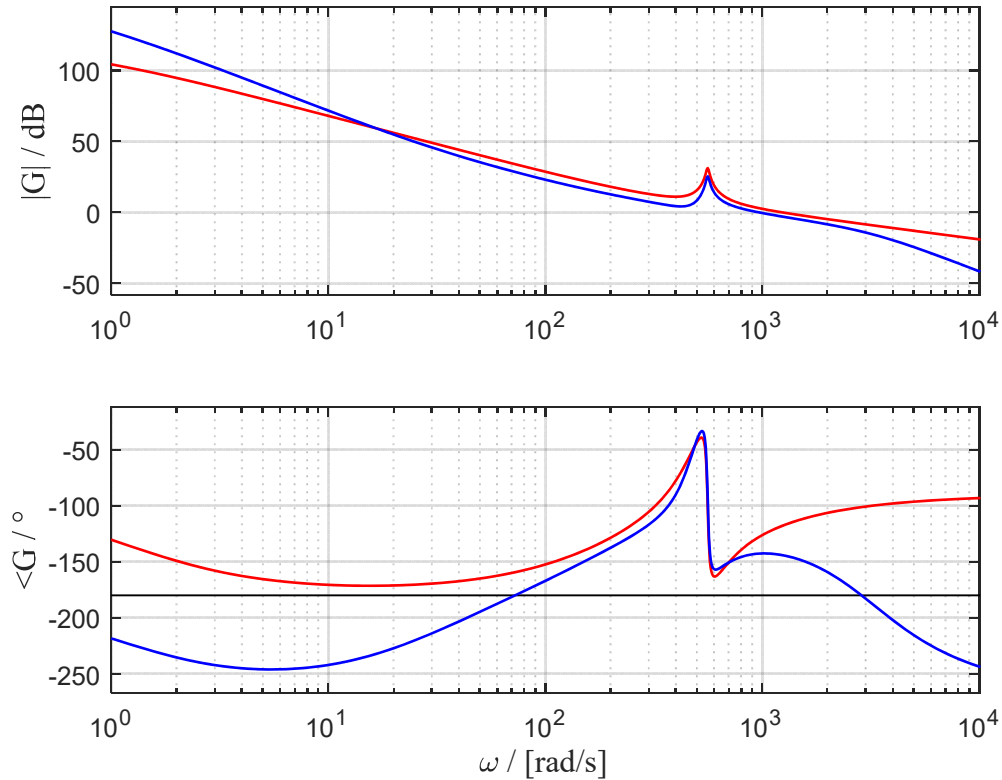


Fig. 2.7 *Open-loop frequency response for system with LQR (red lines) and LQG compensator (blue lines)*

The robustness of the nonlinear control system against nonlinear plant characteristics like friction, saturations, tacho ripple as well as quantization, and against plant parameter variations has been checked by closed-loop simulation. As will be shown with the experimental results, this allowed a very good prediction of the real system behavior.

3. Control implementation and results

Since the above compensator has been designed in the continuous time domain, its differential equations have to be discretized for digital implementation. A very straightforward option is to discretize the dynamic subsystems of the compensator, i.e. the weighting model in the regulator and the state space model of the estimator, by using appropriate discretization methods. To check for the discretization and nonlinear implementation effects before starting with the real experiment, the discrete compensator has been closed-loop simulated with the continuous nonlinear plant model of the EMPS from section 1 which includes additional blocks for the signal interfaces. The corresponding Simulink block diagram is shown in Fig. 3.1. To correct the offset and gain error in the real tachometer signal, a signal condition subsystem [15] is added to the control. The simulation results show a remarkable robustness of the control system against process and measurement noise as well as plant uncertainties, like a varying stiffness c_{dl} of the coupling between the drive and load side, a varying load-side inertia J_l and changing friction characteristic. A sampling rate of 4 kHz turned out to produce satisfying, quasi-continuous results.

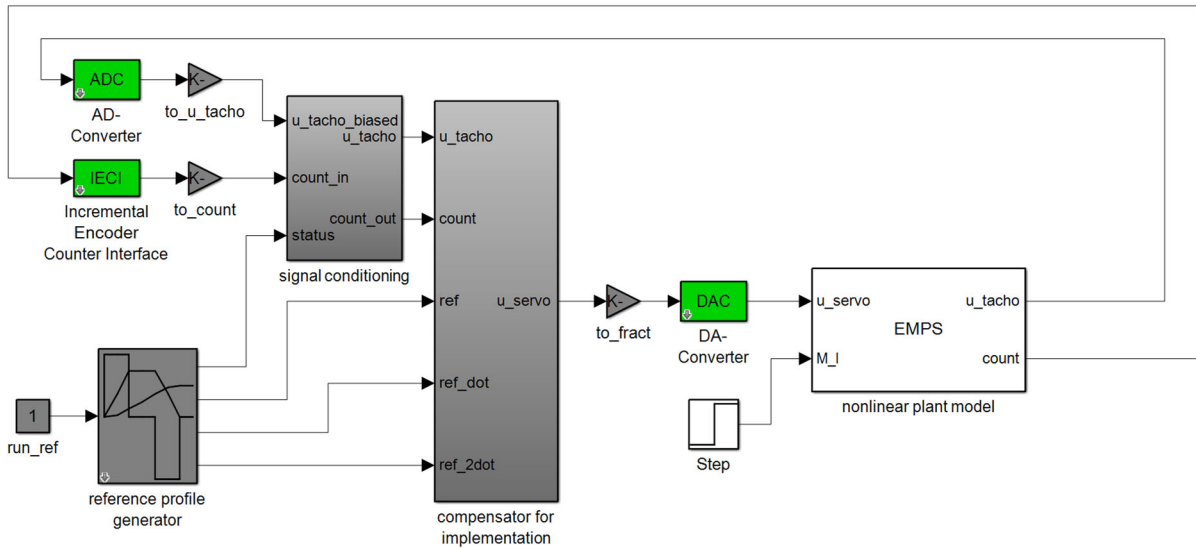


Fig. 3.1 Block diagram for nonlinear control system analysis by closed-loop simulation

For rapid control prototyping, the compensator as well as the signal conditioning, reference profile generator and interfacing blocks from Fig. 3.1 have been copied to the block diagram in Fig. 3.2 that has been augmented by additional blocks for encoder index search (homing) as well as operational and safety provisions. The used total development environment [3] allowed a seamless transition to the experiment by automatic code generation, experiment control and data acquisition.

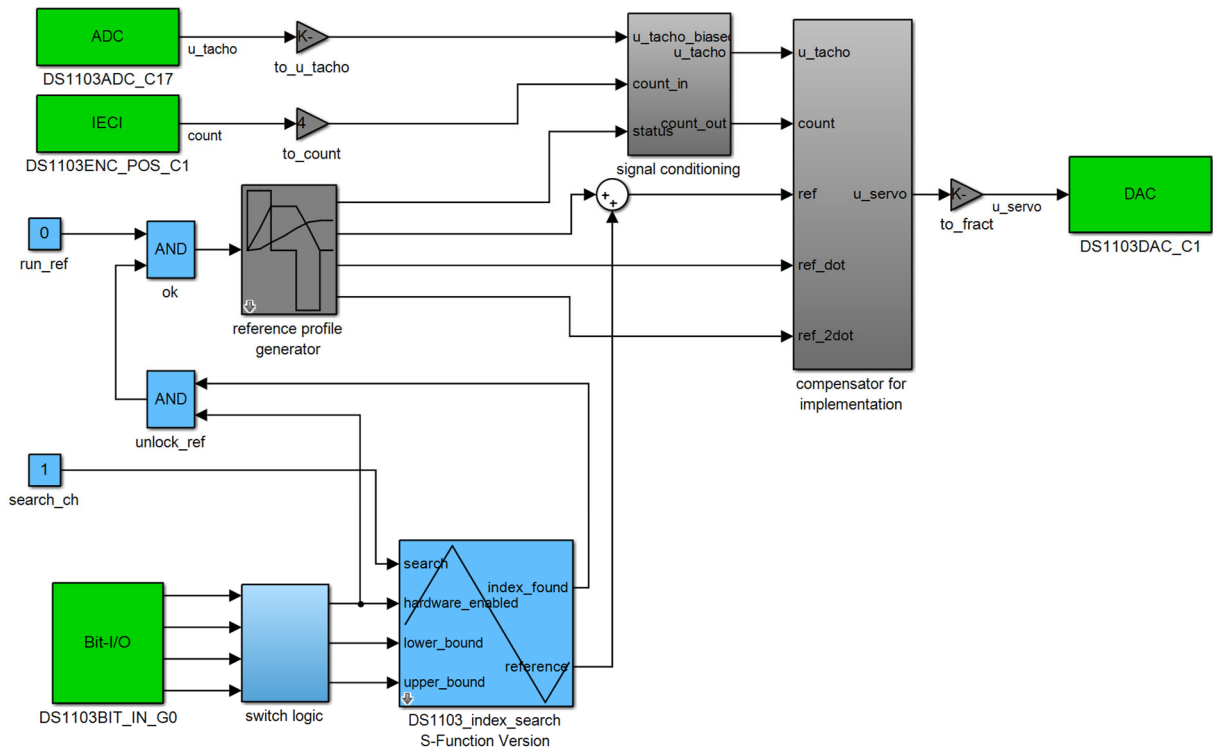


Fig. 3.2 Block diagram for control implementation by automatic code generation

A simulation result for the reference motion of the carriage, which is depicted in Fig. 3.3 and commanded to the control, is presented by the position error and control signal measurements in Fig. 3.4.

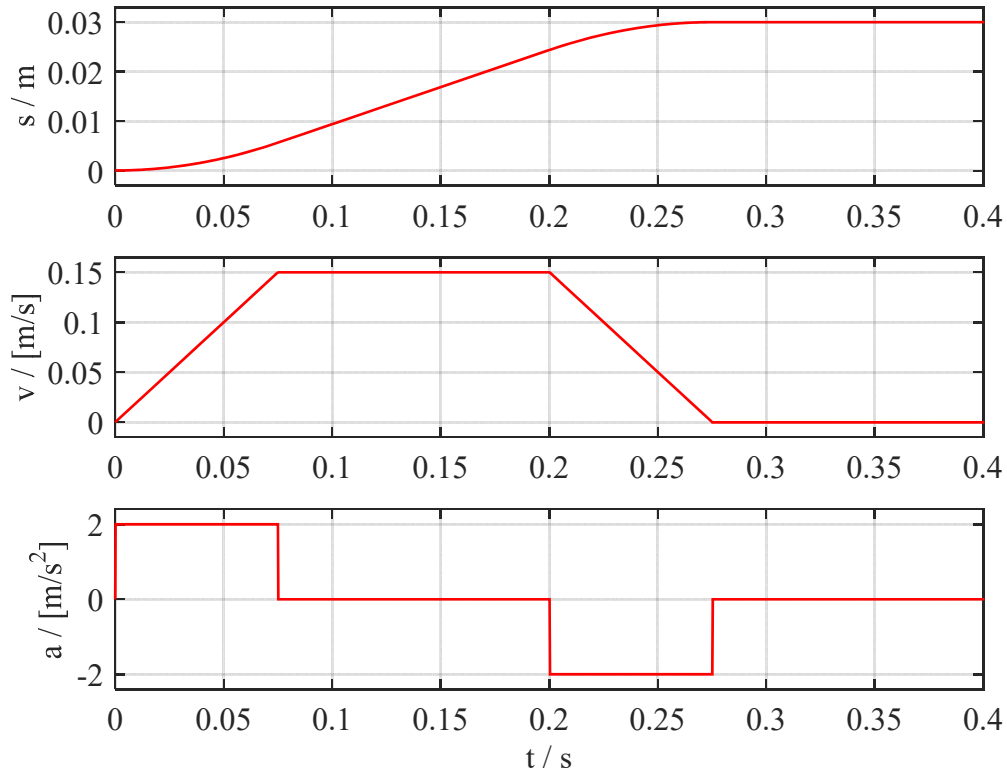


Fig. 3.3 Carriage reference position (top), velocity (middle) and acceleration (bottom) from reference profile generator

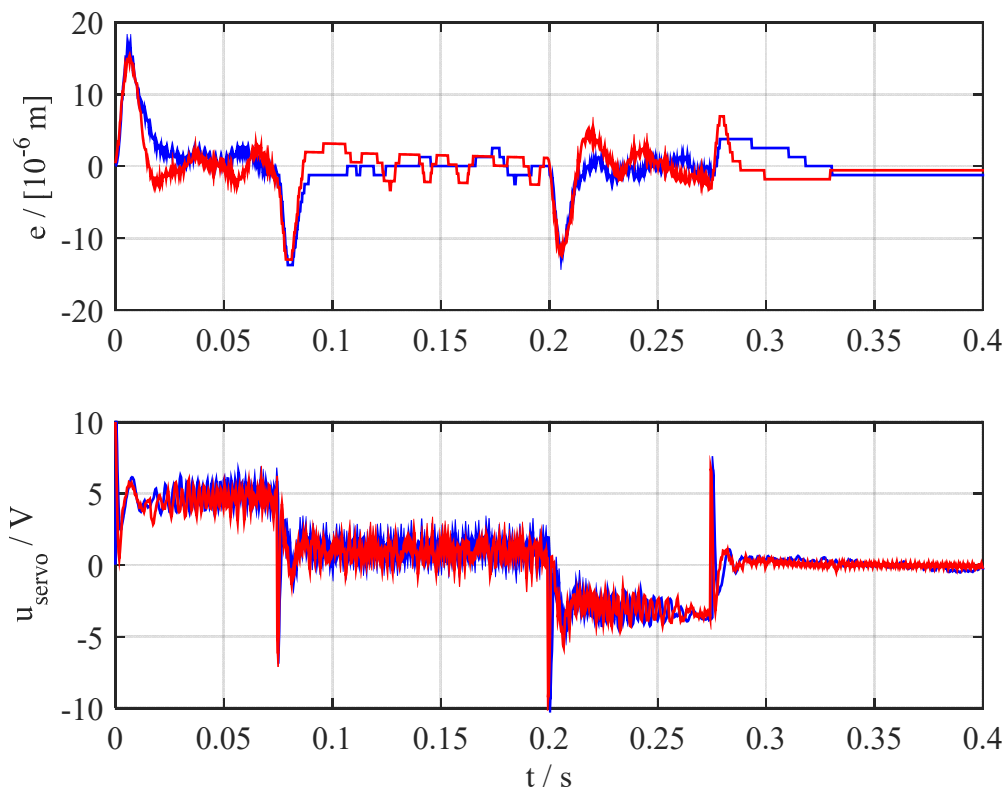


Fig. 3.4 Position error (top) and control signal (bottom) from measurement (red lines) and simulation (blue lines)

The steps in the acceleration command produce a control signal close to the saturation bounds of the servo amplifier of ± 10 V. Despite this strong reference excitation, due to a high control bandwidth, the maximum position error is less than 20 μm and the error settling times are about 10 ms. Vibrations from the flexible coupling between drive and load side are actively damped by the control. The control shows significantly better results than with the simpler compensator from [6], standard single-loop PID or P-PI cascade control [5]. Finally, the feedforward of the disturbance estimate from the estimator and the high control bandwidth yield a strong rejection to external force or torque inputs F_I or M_I , which becomes evident in the experiment when one tries to twist the screw manually.

4. Conclusions

As shown for the EMPS, a LQG control provides very good results in high speed and precise position control. This is achieved by a systematic approach in the control design including a modelling of the deterministic and stochastic reference and disturbance environment of the plant and a modelling of the design objectives specified by the control engineer. The objective variables used in the LQR cost function, suitable weightings derived from the actual and desired variable bounds as well as a rule to determine meaningful noise intensity matrices for the LQE design from sensor and signal interface specifications are crucial for a straightforward design procedure. Robustness of the linear control system with the resulting LQG compensator can be achieved by aspiring LTR with appropriate process noise intensities in the LQE design. Further robustness analysis for the nonlinear control system and investigation of implementation effects have to be performed by simulation.

With the contemporary software tools for design and simulation, the above systematic approach can be very well guided by design template files and a small graphical user interface [5]. A total development environment for rapid control prototyping and experimentation allows a seamless transition to the experiment and concept proving. With the knowledge of the basic theory, one can easily develop advanced control concepts in a minimum of time. The LQG control design for the EMPS can be seen as a sample for this.

References

- [1] B. Friedland, Control System Design. McGraw-Hill, 1986.
- [2] F. L. Lewis, Applied Optimal Control and Estimation. Prentice-Hall, Englewood Cliffs, NJ, USA, 1992.
- [3] H. Hanselmann, DSP in Control: The Total Development Environment. International Conference on Signal Processing Applications & Technology ICSPAT'95, Boston, MA, USA, October 24-26, 1996.
- [4] D. Weiske, Modellbildung für einen Positionierantrieb mit Reibung und Elastizität. Thesis for diploma degree at Cologne Laboratory of Mechatronics, Faculty of Automotive Systems and Production, Cologne University of Applied Sciences, 1996.
- [5] H. Henrichfreise, Practical Issues on Classical and Modern Control of Electromechanical Drive Systems. Seminar at Conference PCIM'93, Nürnberg, Germany, June 21, 1993.
- [6] H. Henrichfreise, Observer based Coulombic friction torque compensation for a position control system. Proceedings of 21st Intelligent Motion Conference PCIM '92, Nürnberg, Germany, April 28-30, 1992.

- [7] R. Kasper, Entwicklung und Erprobung eines instrumentellen Verfahrens zum Entwurf von Mehrgrößenregelungen. Fortschritt-Berichte VDI, Reihe 8, Nr. 90, VDI-Verlag, Düsseldorf 1985.
- [8] J. Lückel and R. Kasper, Optimization of the disturbance and reference characteristics of linear, time-invariant systems by stationary compensation of unstable excitation models. *Int. Journal of Control*, No 41, 1985, pp. 259-269.
- [9] M. Wieland, Untersuchung des Einflusses einer dynamischen Bewertung der Entwurfszielgrößen beim LQR-Entwurf für eine Positionierregelung. Thesis for diploma degree at Cologne Laboratory of Mechatronics, Faculty of Automotive Systems and Production, Cologne University of Applied Sciences, 1996.
- [10] A. Grace, A. J. Laub, J. N. Little and C. Thompson, Control System Toolbox User's Guide. The MathWorks, Inc., Natick, Mass. 01760, October 30, 1990.
- [11] A. J. Laub, A Schur Method for Solving Algebraic Riccati Equations. *IEEE Trans. on Automatic Control*, Vol. AC-24, 1979, pp. 913-921.
- [12] A. V. Oppenheim and R. W. Schaffer, Digital signal processing. Prentice-Hall, 1975.
- [13] J. C. Doyle and G. Stein, Robustness with Observers. *IEEE Trans. on Automatic Control*, Vol. AC-24, 1979, pp. 607-611.
- [14] H. Hanselmann, Implementation of Digital Controllers - A Survey. *Automatica*, Vol. 23, No. 1, 1987, pp. 7-32.
- [15] H. Henrichfreise and C. Witte, CAE-Supported Design and Testing of a Signal Conditioning Subsystem for Analog Velocity Measurement in Position Control Applications. 7th German-Polish Seminar, University of applied sciences Cologne, May 8-14, 1995.